ORIGINAL ARTICLE

# Biomechanical comparison of alternative densities of pedicle screws for the treatment of adolescent idiopathic scoliosis

Xiaoyu Wang · Carl-Eric Aubin · Isabelle Robitaille · Hubert Labelle

**Abstract**

*Purpose* The objective of this computational study was to compare the biomechanical effects of different implant densities in terms of curve reduction and the force levels at the implant–vertebra interface and on the intervertebral elements.

*Methods* Eight cases were randomly picked among patients who have undergone a posterior spinal instrumentation for adolescent idiopathic scoliosis (AIS). For each case, two computer simulations were performed, one with the actual surgery implant pattern and another with the same fusion levels but an alternative implant pattern proposed by an experienced surgeon. The two implant patterns for each case were respectively put into higher and lower implant density group. The spinal correction and the force levels at bone–implant interface and on the intervertebral elements were analyzed and compared between the two groups.

*Results* There were on average 13% more pedicle screws and 30% more bilaterally placed pedicle screws in the higher versus lower density group. The difference in the density of screws (92% vs. 79%) did not lead to significant difference in terms of the resulting main thoracic (MT) Cobb angle, and the MT apical axial vertebral rotation. The average and maximum implant-vertebra force levels were about 50 and 65%, respectively higher in the higher versus lower density group, but without consistent distribution patterns. The average intervertebral forces did not significantly differ between the two groups.

*Conclusions* With the same fusion levels, lower density screws allowed achieving similar deformity correction and it was more likely to have lower screw–vertebra loads.

## Introduction

Surgical instrumentation is the main option for the treatment of severe spinal deformities [1, 2]. Over the last two decades, tremendous progress has been made in segmental spinal instrumentation [3, 4]. One of the remarkable developments was the introduction of pedicle screws which, using the strongest part of the vertebra for anchoring the implant, have greatly improved the stability of spinal instrumentation and allowed surgeons to apply higher corrective forces to translate and derotate the scoliotic spine [5, 6]. Basic deformity reduction techniques associated with the modern segmental spinal instrumentation systems for posterior spinal fusion involve vertebral translation, rod derotation, apical vertebral derotation, bilateral apical vertebral derotation, direct vertebra derotation, compression and distraction, and in situ rod contouring [7, 8]. In order to apply certain correction techniques and to have a better control on the deformed spine, there has been a noticeable trend among spine surgeons to use more and more pedicle screws [9–11]. Nowadays, pedicle screws are frequently placed bilaterally at each vertebra included in the fusion, but some surgeons

X. Wang · C.-E. Aubin (✉) · I. Robitaille
Department of Mechanical Engineering, Ecole Polytechnique de Montréal, P.O. Box 6079, Downtown Station, Montreal, QC H3C 3A7, Canada
e-mail: carl-eric.aubin@polymtl.ca

C.-E. Aubin · I. Robitaille · H. Labelle
Research Center, Sainte-Justine University Hospital Center, 3175, Cote Sainte-Catherine Road, Montreal, QC H3T 1C5, Canada

recommend fewer screws [12]. In spite of the demonstrated benefits of pedicle screws, the associated complications, risks, and the hardware costs are not negligible [13, 14]. Several clinical studies have been carried out to compare the deformity-correction effects of spinal instrumentations with the same fusion levels but different number (density) of implants [9–11]. Studies have also been conducted to evaluate intervertebral and implant-vertebra force levels [15]. However, systematic biomechanical studies have yet to be done in order to improve knowledge on the effects of the total number of implants on curve corrections and resulting stress levels.

The objective of this computational study was to analyze and compare the biomechanical effects of alternative densities of pedicle screws for the treatment of adolescent idiopathic scoliosis (AIS) in terms of curve reduction and the resultant force levels at the implant–vertebra interface and on the intervertebral elements. The tested hypothesis was that increasing the number of implants allows supplementary deformity correction, but tends to overconstrain the instrumented scoliotic spine, therefore creating high stresses at the bone-implant interface.

## Methods

A numerical computer simulation platform was developed to simulate the biomechanical effects of patient-specific spinal instrumentation. Using the developed computer simulation software, the posterior spinal instrumentations of eight patients with AIS having previously undergone posterior instrumentation and fusion were simulated first with the actual surgical instrumentation configurations and major corrective maneuvers. Then, the instrumentations with alternative configurations proposed by an experienced surgeon (HL) were simulated, for which corrective maneuvers and all parts of the numerical models were identical, except for the total number of implants. The next sub-sections detail the modeling and simulation methods.

### Computer biomechanical model for patient-specific spinal instrumentation

The three-dimensional (3D) geometric model of the scoliotic spine of each subject with AIS was created using a 3D reconstruction technique [16]. Pre-operative postero-anterior and lateral radiographs were taken with the patient wearing a small calibration plate on their back. On the two numerical radiographs, markers on the calibration plate were detected. Then, 14 anatomical landmarks (tips of the pedicles, vertebral body corners, and endplate centers) were identified on each vertebra and their 3D coordinates computed using 3D reconstruction and

optimization algorithms [16]. With the prior knowledge of each vertebra's topology, a predefined detailed 3D vertebral model was registered using the fourteen anatomical landmarks and an optimization technique [16]. This 3D reconstruction technique allows an average 3.3 mm accuracy for the entire vertebrae ($1.2 \pm 0.8$ mm for the landmarks of the vertebral bodies and $1.6 \pm 1.1$ mm for the pedicles) [17].

During the simulation of the surgical instrumentation, the deformation of each vertebra being far smaller than the intervertebral displacement, each vertebra was considered as a rigid body using the reconstructed geometry. The spinal segment from T1 to pelvis was then modeled as a set of rigid vertebral parts coupled by flexible elements (representing the intervertebral disks, ligaments and facet joints). The load–displacement relation of each of these flexible elements was initially defined using the previously reported experimental results [18, 19] and then adjusted to account for the patient specific spinal geometry [20] and stiffness [21, 22]. This method of spine modeling has been previously validated by simulating posterior spinal instrumentation of ten scoliotic patients with AIS; the observed differences were generally below 5° for the Cobb angles in the frontal and sagittal planes [21].

During surgical instrumentation, the deformation of each individual implant (screw or hook) being negligible compared to the intervertebral displacement; each implant was modeled as a rigid body. The rod was modeled as a flexible beam with the mechanical properties of the rod material used in the surgery. The vertebra–implant connections were modeled as a generalized non-linear spring that restrained the relative motion between the implant and the vertebra in both rotation and translation. The stiffness coefficients were approximated using in-house experimental data on cadaveric instrumented vertebrae, but its parametric formulation allows using more detailed data when available in the future.

### Numerical case simulations

Eight cases were randomly picked among patients who have undergone a posterior spinal instrumentation for AIS over the past 9 years at Sainte-Justine University Hospital Center. The collected information necessary to define the simulations included:

- Pre-operative coronal and lateral radiographs with calibration markers,
- Pre-operative left and right bending radiographs,
- Implant and rod material, and geometric parameters and their mechanical properties,
- Instrumentation configurations (implant type, location, and rod shape),

**Table 1** Patient information

| Case no. | Sex | Age | Height (cm) | Weight (kg) | Lenke classification |
|---|---|---|---|---|---|
| 1 | Female | 12 | 162 | 43 | 1A |
| 2 | Female | 15 | 167 | 56 | 3C |
| 3 | Female | 13 | 155 | 43 | 1C |
| 4 | Female | 17 | 178 | 66 | 1A |
| 5 | Female | 16 | 156 | 49 | 2A |
| 6 | Female | 15 | 165 | 52 | 3C |
| 7 | Female | 19 | 162 | 47 | 4B |
| 8 | Female | 15 | 165 | 51 | 1B |

- Correction maneuver documentation,
- Postoperative coronal and lateral calibrated radiographs.

Patient information and the geometric indices computed from the reconstructed pre-operative 3D spinal models are presented in Tables 1 and 2.

For each case, two simulations were performed, one with the same surgical configuration used and another with an alternative configuration proposed by an experienced surgeon. Depending on the total number of implants, the two configurations for each case were respectively classified into higher density implant group and lower density implant group. As an example, Table 3 shows the lower and higher density implant configurations for case 4.

In this study, only the basic corrective maneuvers were simulated, i.e., the rod attachment, rod derotation, and compression/distraction. To simulate the rod attachment maneuver, displacement constraints in translation and

**Table 3** Two instrumentation configurations for case 4

| Lower density implant configuration | | | Higher density implant configuration | | |
|---|---|---|---|---|---|
| | Left | Right | | Left | Right |
| T1 | | | T1 | | |
| T2 | | | T2 | | |
| T3 | TPH | TPH | T3 | TPH | TPH |
| T4 | MOS | MOS | T4 | MOS | MOS |
| T5 | | | T5 | MOS | MOS |
| T6 | | | T6 | MOS | MOS |
| T7 | | | T7 | MOS | MOS |
| T8 | MOS | MOS | T8 | MOS | MOS |
| T9 | MOS | MOS | T9 | MOS | MOS |
| T10 | MOS | MOS | T10 | MOS | MOS |
| T11 | | | T11 | MOS | MOS |
| T12 | | | T12 | MOS | MOS |
| L1 | MOS | MOS | L1 | MOS | MOS |
| L2 | MOS | MOS | L2 | MOS | MOS |
| L3 | | | L3 | | |
| L4 | | | L4 | | |
| L5 | | | L5 | | |

*TPH* transverse process hook, *MOS* monoaxial (fixed) pedicle screw

rotation were created between the segment of the rod and the targeted implants. Cylindrical joints were then introduced to connect the implant to the rod. For the rod-derotation maneuver, a torque was gradually applied on the rod up until its profile was parallel to the sagittal plane. As the rod was derotated, the implants were free to slide and rotate along the rod central axis. The compression/

**Table 2** Geometric indices computed from the reconstructed pre-operative 3D spinal models

| Case no. | MT Cobb end-apex-end | TL/L Cobb end-apex-end | Kyphosis (T4–T12) | Lordosis (L1–L5) | MT apical axial rotation |
|---|---|---|---|---|---|
| 1 | 83° | 12° | 54° | 12° | −4° |
| | T6, T10, L1 | L1, L3, L5 | | | |
| 2 | 56° | 29° | 40° | 16° | −1° |
| | T6, T9, T11 | T11, L1, L5 | | | |
| 3 | 35° | 30° | 18° | 5° | −6° |
| | T7, T11, L2 | L2, L3, L5 | | | |
| 4 | 51° | 32° | 34° | 27° | −23° |
| | T7, T10, L1 | L1, L3, L5 | | | |
| 5 | 64° | 10° | 66° | 32° | −2° |
| | T5, T8, T11 | T11, L2, L5 | | | |
| 6 | 61° | 72° | 42° | 34° | −14° |
| | T5, T8, T11 | T11, L2, L5 | | | |
| 7 | 51° | 40° | 42° | 27° | −18° |
| | T5, T8, T11 | T11, L3, L5 | | | |
| 8 | 40° | 39° | 33° | 32° | −10° |
| | T5, T9, T12 | T12, L3, L5 | | | |

*MT* main thoracic, *TL/L* thoraco-lumbar/lumbar

distraction maneuver was simulated by gradually applying a force between the two identified implants up until a specified distance was achieved.

For the two simulations of each case, the biomechanical models of the spine, the boundary conditions, the diameter, shape and mechanical properties of the rods, the placement of the implants which are common for the two simulations, as well as the correction maneuvers, were all identical. The only difference was the number of implants between the lower and higher density implant configurations.

After each simulation, each intervertebral force and each implant-vertebra force were computed. The former was the resultant force between vertebrae while the later was the resultant force applied by an implant on its anchored vertebra. The spinal geometric indices were computed using the 3D geometric model of the simulated instrumented scoliotic spine (main thoracic (MT) Cobb angle, Kyphosis, Lordosis, and the MT apical axial vertebral rotation).

## Results

Compared to the lower density implant group, an instrumentation configuration in the higher density implant group used, on average, six more implants, 13% more pedicle screws, and 30% more bilaterally instrumented vertebrae (Table 4).

This difference in implant density did not lead to significant differences in terms of the resulting MT Cobb angle in the coronal plane (Table 5), with differences not exceeding 3° for all the eight cases. For the axial rotation in the transverse plane at the apex of the main thoracic curve, the absolute values of the differences did not exceed 4° for all cases except for case 1 which is 8°.

On average, the resultant implant–vertebra forces for the higher density implant group were about 50% higher than the lower density implant group (Table 6). This difference varied from case to case: in two cases the lower density configuration gave higher resulting average forces while in six cases the higher density configuration resulted in higher resulting average forces. For six of the eight cases, the maximum resultant implant-vertebra force in the higher density implant group was higher than in the lower density implant group, indicating a higher risk of implant–vertebra interface loosening or implant pullout failure (Table 6). Statistically, the mean implant-vertebral force level of the higher density implant group is significantly higher than the lower density group ($p < 0.05$).

In terms of the average intervertebral force level, the lower density implant configuration is higher than the

**Table 4** Summary on implant density

| | Lower density implant group | Higher density implant group |
|---|---|---|
| Average number of implants (min–max) | 15 (12–19) | 21 (17–24) |
| Percentage of instrumented vertebrae between the UIV and LIV (min–max) | 78% (58–100%) | 97% (85–100%) |
| Percentage of implants (left/right) | 56/44% | 53/47% |
| Percentage of bilaterally instrumented vertebrae | 54% (31–73%) | 84% (62–100%) |
| Percentage of pedicle screws/total implants | 79% | 92% |

**Table 5** Geometric indices: lower density (LD) group simulation results and higher density (HD) group simulation results

| Case no. | MT Cobb | | MT apical axial rotation | | Kyphosis (T4–T12) | | Lordosis (L1–L5) | |
|---|---|---|---|---|---|---|---|---|
| | HD | LD | HD | LD | HD | LD | HD | LD |
| 1 | 19° | 19° | −6° | −14° | 40° | 42° | 3° | 9° |
| 2 | 7° | 7° | −6° | −4° | 41° | 33° | 13° | 11° |
| 3 | 8° | 7° | −7° | −3° | 22° | 24° | 7° | 9° |
| 4 | 12° | 9° | −11° | −13° | 30° | 23° | 18° | 13° |
| 5 | 7° | 6° | −5° | −9° | 42° | 50° | 26° | 27° |
| 6 | 8° | 7° | −18° | −18° | 35° | 25° | 22° | 28° |
| 7 | 12° | 11° | −26° | −23° | 47° | 44° | 22° | 22° |
| 8 | 16° | 17° | −6° | −7° | 27° | 27° | 29° | 32° |
| Average | 16.2° | 14.9° | −11.2° | −10.5° | 33.4° | 35.5° | 18.7° | 17.5° |
| (p values) | (0.128) | | (0.333) | | (0.180) | | (0.184) | |
| Average difference (std) | 1° | (1°) | −1° | (4°) | −2° | (6°) | 1° | (4°) |

**Table 6** Average intervertebral and implant-vertebra force level comparison: mean (min – max) (in Newton)

| Case no. | Intervertebral force magnitude | | Implant-vertebra force magnitude | |
|---|---|---|---|---|
| | Lower density implant group | Higher density implant group | Lower density implant group | Higher density implant group |
| 1 | 172 (31–359) | 185 (27–399) | 295 (0–750) | 195 (0–733) |
| 2 | 167 (24–599) | 143 (9–447) | 90 (4–483) | 337 (0–798) |
| 3 | 179 (15–442) | 121 (15–354) | 243 (0–659) | 414 (99–993) |
| 4 | 188 (7–486) | 185 (9–573) | 172 (0–755) | 218 (0–837) |
| 5 | 213 (10–521) | 259 (11–560) | 225 (0–859) | 353 (0–1133) |
| 6 | 251 (17–523) | 228 (13–604) | 137 (0–491) | 240 (0–747) |
| 7 | 138 (6–596) | 157 (4–580) | 290 (0–1432) | 275 (0–1193) |
| 8 | 122 (9–302) | 165 (9–615) | 140 (0–459) | 282 (0–1086) |
| Avg. | 179 | 180 | 199 | 289 |
| Std. | 41 | 45 | 76 | 74 |
| Comparison (p values) | 0.451 | | 0.027 | |
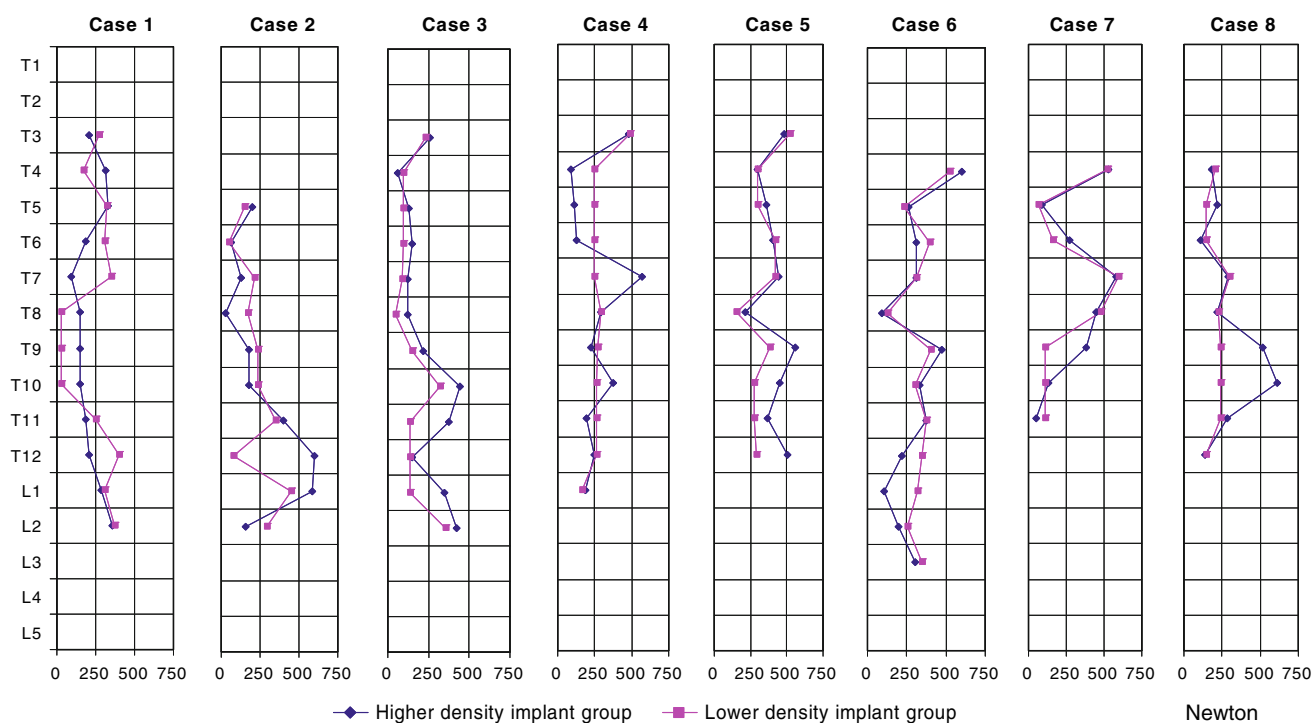


**Fig. 1** Intervertebral force level comparison (in Newton)

higher density configuration in half of the eight cases. Statistically, the difference between the means of the two groups was not significant ($p < 0.05$).

There were significant resultant implant–vertebra force differences between the two groups at the local levels (Figs. 1, 2). For instance, the difference between the intervertebral force magnitudes at T7–T8 level for case 4 was about 260 N (Fig. 1) and the difference between the

implant-vertebra force magnitudes on the left side of T8 for case 1 was about 370 N (Fig. 2).

## Discussion

Case simulations have demonstrated that for the same fusion levels, rod shape and material, and using the same

**Fig. 2** Implant-vertebra force level comparison (in Newton). At each level, the higher/lower density forces are presented for the right (negative values) and left (positive values) sides
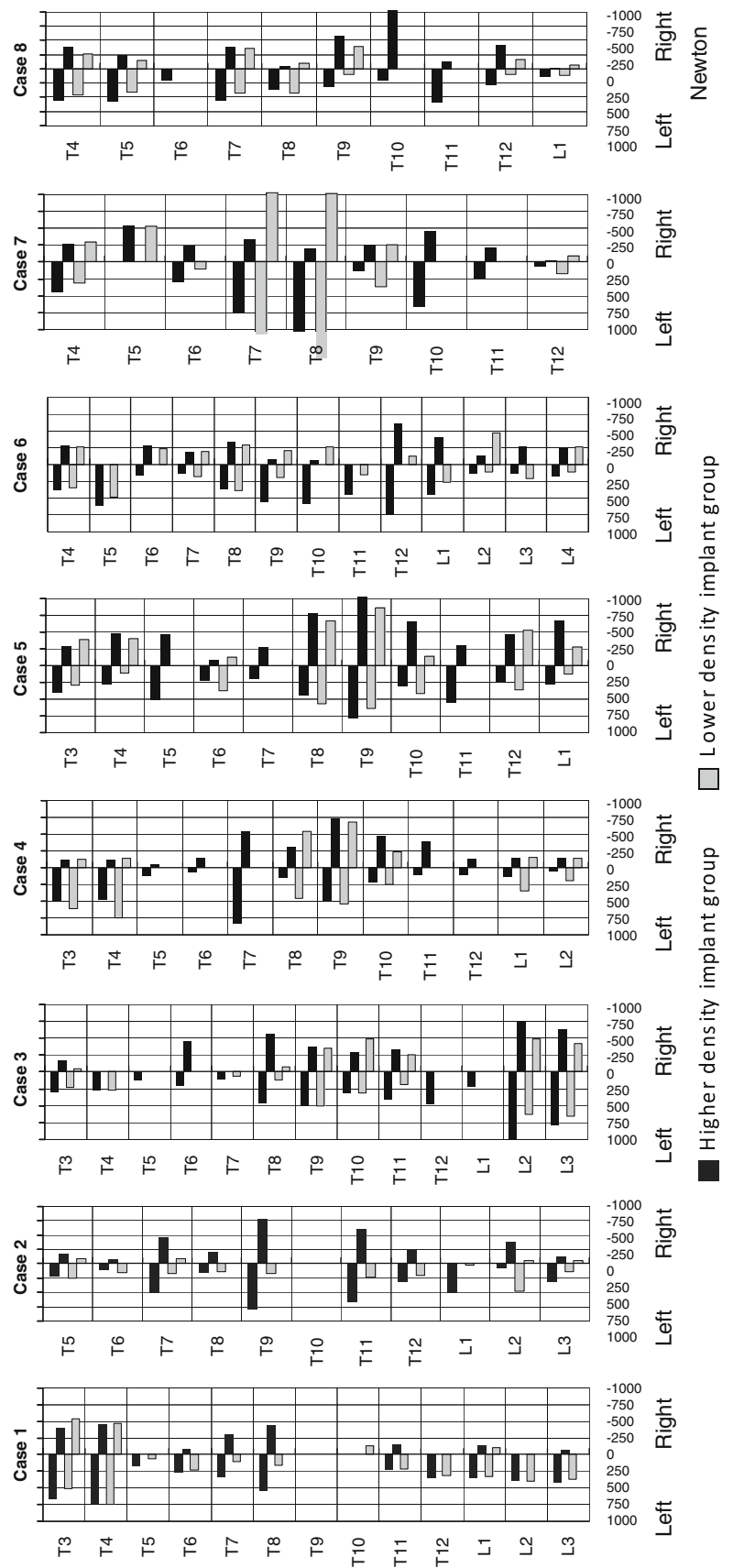
basic correction maneuvers, increasing the number of implants does not result in improved scoliosis deformity correction (in the coronal plane). This finding agrees well with previous clinical reports [9, 12] suggesting that interval pedicle screw placement constructs seem to be equally effective as consecutive constructs for facilitating curve correction in patients with Lenke 1 AIS [12]; higher implant density did not improve curve correction for patients with AIS operated by a single surgeon using an identical surgical technique and type of instrumentation [9]. However, a significant correlation has been found between the number of implants and the curve correction using a multi-center database of AIS patients [11]. It has also been reported that increasing the number of implants can improve the correction of curves with higher stiffness, as determined by the fulcrum bending radiograph [10]. The discrepancies between the results of this work and the clinical studies may be explained by the fact that there exist considerable differences on how the increased control provided by adding additional implants have been explored. An increased number of implants theoretically provide more control on the deformed spine for performing verte-bral derotation and compression/distraction on more ver-tebral levels. However, the available number of degrees of freedom provided by the screw-rod connection may not allow easily applying the desired maneuvers leading to overconstraints (extra forces). Therefore, this additional control was not taken into account in this study. The dis-crepancies among clinical studies may also be attributed to the surgeon-specific objectives [23] and techniques [24, 25]. With the recent advances in correction techniques, some surgeons prefer the additional control on the deformed spine, while others much less.

Compared to the coronal plane, the difference between the lower and higher density groups on the sagittal and transverse planes were fairly noticeable with standard deviations between 4° and 6°. This variability may be explained by supplementary constraints introduced by the additional connections, especially when the screws were not perfectly aligned. It has been demonstrated that slight variations of screw insertion point and screw trajectory affect the curve correction and have a significant effect on the resulting forces at bone–screw interface especially with monoaxial (fixed) screws [15]. However, due to the rela-tively small number of cases, no general conclusion can be made regarding the optimal pedicle screw density and the resulting effects on the sagittal and transverse planes associated with basic correction maneuvers.

At the bone–implant interface and on the intervertebral elements, no correlation was found between the individual force level and the implant density. This can be explained by the fact that the force level is determined by a number of factors, and is highly sensitive to implant placement when

monoaxial screws are involved [15]. Increased screw density lead to decreased average bone-screw load for two of the eight cases, while for the rest of the cases, higher average bone-screw load was observed. The average implant-vertebra force magnitude of all cases in the higher density implant group was significantly higher. This can be explained by looking into the screw placement variation and how screw attachment works with monoaxial pedicle screws. Considering the complexity of pedicle anatomy, pedicle screw insertion could be mentally and technically demanding [26, 27]. The priority is to make sure that each screw is contained solely in the desired pedicle and its alignment with its neighbors often comes after this priority [27–29]. Even with computer-assisted image-guided tech-niques, there is considerable variation in the placement of each pedicle screw with respect to its neighbors. For screw insertion depth, variation of 2–4 mm has been reported in screw placement studies [28]. Variation in screw insertion orientation is also significant, sometimes with pedicle violation (medial, inferior, superior, and anterolateral ver-tebral body) [27]. Variation of coronal plane screw position greater than 2 mm was reported (distance between medial pedicle wall and medial margin of the pedicle screw and between lateral margin of the pedicle screw and lateral vertebral corpus) [29]. The final positions of all screw head slots are therefore unlikely to be perfectly smoothly aligned. Depending on the screw-to-rod connection mecha-nism, this screw malalignment is transformed into adverse bone-screw forces of different magnitudes when various connection maneuvers are performed [15, 30, 31].

Although monoaxial pedicle screws have demonstrated certain superiority for vertebral rotation correction, they have a potential disadvantage arising from the difficulty in achieving adequate seating of the rod into the screw head saddle [30]. Any malalignment between the rod and the fixed-angle screw head could overconstrained the instru-mented spine and result in additional stress (not beneficial to deformity correction) on the bone–screw interface as the rod is seated into the screw saddle and the locking mech-anism firmly attaches the screw to the rod [31].

Due to the pedicle screw placement variation and the drawbacks of screw-to-rod connection mechanism of monoaxial pedicle screws, the higher the screw density the more the whole system is overconstrained and the more likely the adverse stresses are put on the bone-screw interface. The above analysis thus explained why the average implant-vertebra force magnitude of all cases in the higher density implant group was significantly higher. The polyaxial screws were designed to provide more freedom on the screw-to-rod connection to facilitate easier rod seating into the screw head saddle. Therefore, polyaxial screws conceptually allow accommodating the screw malalignment in the coronal plane and lower bone-screw

loads are expected compared with monoaxial screws. When screw density is relatively high and bone-screw load is of major concerns, e.g., for patients with large and stiff spinal deformities or for patients with compromised bone quality or osteoporosis, polyaxial screws seem to offer better perspective for safer spinal instrumentation. To what extent the polyaxial screws can help reduce bone-screw loads remains to be investigated and is out of the scope of this paper.

In this study, only basic deformity correction maneuvers were simulated, i.e., vertebral translation by rod attachment, rod derotation, and compression/distraction. The difference obtained by increasing the number of implants could have been more significant if other deformity correction maneuvers had been simulated, such as direct vertebral derotation, apical vertebral derotation, bilateral apical vertebral derotation, and in situ rod contouring.

Fewer implants globally increase the load on each implant, but reduce the overconstraints and supplementary stresses exerted on the vertebral column. More implants improve the ability to share the loads and apply local correction maneuvers, but at the expenses of overconstraints resulting in higher stresses on the construct. The optimal trade-off between having more control for local correction and reducing the risk of higher stresses at the bone–implant interface has yet to be systematically studied.

## Conclusion

No significant difference was observed between the higher and the lower density implant configurations with respect to scoliosis deformity correction in the coronal plane (i.e., similar correction can be achieved with less implants) when simulating basic corrective maneuvers (i.e., vertebral translation by rod attachment and rod derotation, and compression/distraction). However, in the sagittal and transverse planes, there was more difference between the lower and higher density groups with standard deviations between 4° and 6°. The difference on the load levels at the bone–implant interface and on the intervertebral elements varied from case to case. On average, however, the lower density implant configurations allowed lower mean implant-vertebra load and similar mean intervertebral load. The maximum implant-vertebra force of the higher density implant group is usually higher than in the lower density implant group. No conclusion can be drawn on the load distribution among implants. The lower density implant configurations generated 31% lower average load on the implant–vertebra interface, but very similar intervertebral forces compared to the higher density implant configurations.

## References

1. Lenke LG, Dobbs MB (2007) Management of juvenile idiopathic scoliosis. J Bone Joint Surg Am 89(Suppl 1):55–63
2. Bridwell KH (1997) Spinal instrumentation in the management of adolescent scoliosis. Clin Orthop Relat Res 335:64–72
3. Lenke LG, Kuklo TR, Ondra S, Polly DW Jr (2008) Rationale behind the current state-of-the-art treatment of scoliosis (in the pedicle screw era). Spine 33:1051–1054
4. Suk SI, Lee CK, Min HJ, Cho KH, Oh JH (1994) Comparison of Cotrel-Dubousset pedicle screws and hooks in the treatment of idiopathic scoliosis. Int Orthop 18:341–346
5. Hamill CL, Lenke LG, Bridwell KH, Chapman MP, Blanke K, Baldus C (1996) The use of pedicle screw fixation to improve correction in the lumbar spine of patients with idiopathic scoliosis. Is it warranted? Spine 21:1241–1249
6. Suk SI, Lee CK, Kim WJ, Chung YJ, Park YB (1995) Segmental pedicle screw fixation in the treatment of thoracic idiopathic scoliosis. Spine 20:1399–1405
7. Johnston CE, Ashman RB, Sherman MC, Eberle CF, Herndon WA, Sullivan JA, King AG, Burke SW (1987) Mechanical consequences of rod contouring and residual scoliosis in sublaminar segmental instrumentation. J Orthop Res 5:206–216
8. Boos N, Aebi M (2008) Spinal disorders: fundamentals of diagnosis and treatment. Springer, Berlin
9. Quan GM, Gibson MJ (2010) Correction of main thoracic adolescent idiopathic scoliosis using pedicle screw instrumentation: does higher implant density improve correction? Spine 35:562–567
10. Cheung KM, Natarajan D, Samartzis D, Wong YW, Cheung WY, Luk KD (2010) Predictability of the fulcrum bending radiograph in scoliosis correction with alternate-level pedicle screw fixation. J Bone Joint Surg Am 92:169–176
11. Clements DH, Betz RR, Newton PO, Rohmiller M, Marks MC, Bastrom T (2009) Correlation of scoliosis curve correction with the number and type of fixation anchors. Spine 34:2147–2150
12. Li M, Shen Y, Fang X, Ni J, Gu S, Zhu X, Zhang Z (2009) Coronal and sagittal plane correction in patients with Lenke 1 adolescent idiopathic scoliosis: a comparison of consecutive versus interval pedicle screw placement. J Spinal Disord Tech 22:251–256
13. Yuan HA, Garfin SR, Dickman CA, Mardjetko SM (1994) A historical cohort study of pedicle screw fixation in thoracic, lumbar, and sacral spinal fusions. Spine 19:2279S–2296S
14. Esses SI, Sachs BL, Dreyzin V (1993) Complications associated with the technique of pedicle screw fixation. A selected survey of ABS members. Spine 18:2231–2238 (discussion 2238–2239)
15. Wang X, Aubin CE, Crandall D, Labelle H (2011) Biomechanical comparison of force levels in spinal instrumentation using monoaxial versus multi degree of freedom postloading pedicle screws. Spine 36:E95–E104
16. Cheriet F, Laporte C, Kadoury S, Labelle H, Dansereau J (2007) A novel system for the 3-D reconstruction of the human spine and rib cage from biplanar X-ray images. IEEE Trans Biomed Eng 54:1356–1358
17. Delorme S, Petit Y, de Guise JA, Labelle H, Aubin CE, Dansereau J (2003) Assessment of the 3-D reconstruction and high-

resolution geometrical modeling of the human skeletal trunk from 2-D radiographic images. IEEE Trans Biomed Eng 50:989–998

18. Panjabi MM, Brand RAJ, White AAI (1976) Three dimensional flexibility and stiffness properties of the human thoracic spine. J Biomech 9:185–192

19. Panjabi MM, Oxland TR, Yamamoto I, Crisco JJ (1994) Mechanical behavior of the human lumbar and lumbosacral spine as shown by three-dimensional load-displacement curves. J Bone Joint Surg Am 76:413–424

20. Gardner-Morse MG, Laible JP, Stokes IAF (1990) Incorporation of spinal flexibility measurements into finite element analysis. J Biomech Eng 112:481–483

21. Aubin CE, Labelle H, Chevrefils C, Desroches G, Clin J, Boivin A (2008) Preoperative planning simulator for spinal deformity surgeries. Spine 33:2143–2152

22. Petit Y, Aubin CE, Labelle H (2004) Patient-specific mechanical properties of a flexible multi-body model of the scoliotic spine. Med Biol Eng Comput 42:55–60

23. Majdouline Y, Aubin CE, Robitaille M, Sarwark JF, Labelle H (2007) Scoliosis correction objectives in adolescent idiopathic scoliosis. J Pediatr Orthop 27:775–781

24. Robitaille M, Aubin CE, Labelle H (2007) Intra and interobserver variability of preoperative planning for surgical instrumentation in adolescent idiopathic scoliosis. Eur Spine J 16:1604–1614

25. Aubin CE, Labelle H, Ciolofan OC (2007) Variability of spinal instrumentation configurations in adolescent idiopathic scoliosis. Eur Spine J 16:57–64

26. Parent S, Labelle H, Skalli W, de Guise J (2004) Thoracic pedicle morphometry in vertebrae from scoliotic spines. Spine 29:239–248

27. Bledsoe JM, Fenton D, Fogelson JL, Nottmeier EW (2009) Accuracy of upper thoracic pedicle screw placement using three-dimensional image guidance. Spine J 9:817–821

28. Amato V, Giannachi L, Irace C, Corona C (2010) Accuracy of pedicle screw placement in the lumbosacral spine using conventional technique: computed tomography postoperative assessment in 102 consecutive patients. J Neurosurg Spine 12:306–313

29. Sarlak AY, Tosun B, Atmaca H, Sarisoy HT, Buluc L (2009) Evaluation of thoracic pedicle screw placement in adolescent idiopathic scoliosis. Eur Spine J 18:1892–1897

30. Lonner BS, Auerbach JD, Boachie-Adjei O, Shah SA, Hosogane N, Newton PO (2009) Treatment of thoracic scoliosis: are monoaxial thoracic pedicle screws the best form of fixation for correction? Spine 34:845–851

31. O'Brien MF, Newton PO (2008) Surgical treatment of adolescent idiopathic scoliosis. In: Kim DH et al (eds) Surgery of the pediatric spine. Thieme Medical Publishers, New York, pp 602–634